Thermal waveguiding in oxide-defined, narrow-stripe, large-optical-cavity lasers

Y. C. Chen, A. R. Reisinger, and S. R. Chinn
Optical Information Systems Incorporated, 350 Executive Boulevard, Elmsford, New York 10523

(Received 8 March 1982; accepted for publication 28 April 1982)

The characteristics of oxide-defined, narrow-stripe large-optical-cavity (LOC) AlGaAs lasers are described. Compared with regular narrow-stripe double heterostructure (DH) lasers, the LOC version exhibits more narrowing of the near-field and far-field distributions, higher astigmatism, higher differential quantum efficiency, and higher incidence of sustained pulsations. We have found that these phenomena can be explained in terms of the formation of a thermal waveguide. There is often a striking similarity in characteristics of narrow-stripe LOC and degraded narrow-stripe DH lasers. We suggest that a thermal waveguiding effect is an important factor in determining the behavior of degraded semiconductor lasers.

PACS numbers: 42.55.Px, 42.60.Da

In this letter, we describe the observation of a thermal waveguide effect in oxide-defined, narrow-stripe large-optical-cavity (LOC) structure lasers. The study is of considerable interest because of the usefulness of LOC structure lasers in high-power applications. A better understanding of the thermal waveguide effect is also important in analyzing and controlling the behavior of gain-guided semiconductor lasers, particularly degraded lasers in which the increasing temperature gradient along the junction plane can considerably influence the waveguiding and dynamic properties of the device.

The structure of the narrow-stripe LOC lasers described in this letter consists of $\sim 1\,\mu$m n-$Al_{0.32}Ga_{0.68}As$, $\sim 1\,\mu$m n-$Al_{0.25}Ga_{0.75}As$, $\sim 0.15\,\mu$m undoped $Al_{0.07}Ga_{0.93}As$, and $\sim 1\,\mu$m p-$Al_{0.33}Ga_{0.67}As$. It differs from the LOC structure originally proposed by Lockwood *et al.*[1] in that the index step between the active layer ($Al_{0.07}Ga_{0.93}As$) and the n-type LOC layer ($Al_{0.25}Ga_{0.75}As$) is still rather large ($\Delta n = 0.18$) in order to achieve low threshold operation. The stripe width is $6\,\mu$. The calculated confinement factor Γ is 0.26 for the fundamental mode and 0.07 for the first order mode. The optical damage power, when driven by 60-ns square pulses, is roughly 300 mW, which is a factor of 2 higher than regular narrow-stripe double heterostructure (DH) lasers with $6\text{-}\mu$ stripe width and $\Gamma = 0.5$. The device parameters of narrow-stripe LOC lasers and regular narrow-stripe DH lasers are summarized in Table I. Compared to a narrow-stripe DH with $\Gamma = 0.5$, the LOC version exhibits considerable near-field and far-field narrowing, very high differential quantum efficiency, highly astigmatic output, and high incidence of self-sustained oscillations, even though the lateral carrier distribution does not seem to be influenced by the additional LOC layer.

Figure 1 shows the power versus current (P-I) characteristics of a narrow-stripe LOC laser under cw and 50-ns pulsed current injection. The unusual feature is that cw operation has lower threshold current and sharper turn-on than pulsed operation. The grossly different characteristics of a narrow-stripe LOC can not be explained by changes in the gain and carrier-induced refractive index profile. These can be deduced from regular narrow-stripe lasers with $\Gamma = 0.5$ and extrapolated for lower confinement factor and higher threshold current.[2] Other waveguiding mechanisms need to

TABLE I. Summary of device parameters of narrow-stripe lasers.

	LOC	Regular DH
Stripe width	$6\,\mu$m	$6\,\mu$m
Confinement factor	0.26	0.5
Differential quantum efficiency (per facet)	40 ~ 60%	20%
Carrier profile FWHM[a]	$10\,\mu$m	$10\,\mu$m
Beam divergence FWHM[b]		
∥	9°	20°
⊥	30°	45°
Near-field FWHM[b]	$8\,\mu$m	$11\,\mu$m
Virtual source FWHM	$1.5 \sim 2\,\mu$m	$< 1\,\mu$m
Astigmatism	$50 \sim 70\,\mu$m	$20 \sim 30\,\mu$m
Percentage of sustained pulsations	60%	rare

[a] Measured at $0.2I_{th}$.
[b] Measured at $1.1I_{th}$.

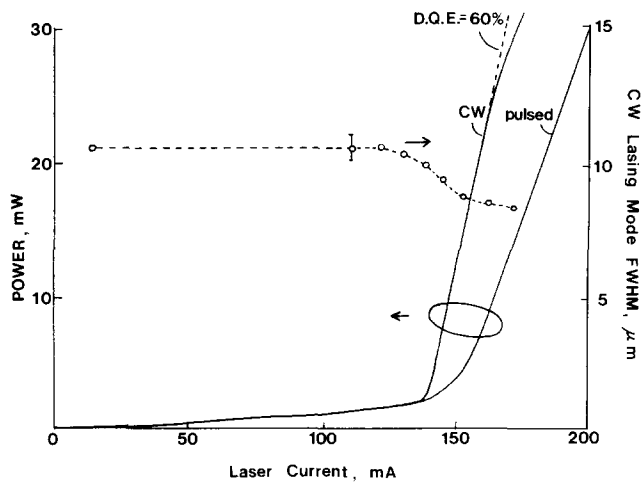

FIG. 1. P-I curves of narrow-stripe LOC laser under cw and 50-ns pulsed current injection. The circles are the cw lasing mode width (FWHM) as a function of current.

 0003-6951/82/02129-03$01.00

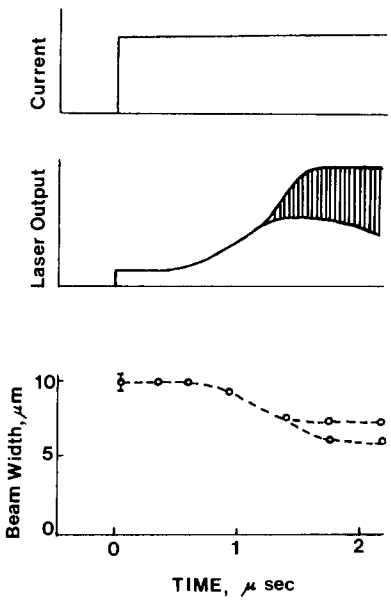

FIG. 2. Pulse response and time-resolved lateral near-field beam width of narrow-stripe LOC laser. The shaded area represents the pulsating laser output. The two branches of the near-field FWHM curve represent data at the maxima (lower branch) and minima (upper branch) of the laser pulsations.

be considered.

We have found that the lateral radius of curvature of the wave front at the facet, calculated from the parameters given in Table I with the assumption of Gaussian beams,[3] is $50\sim70\,\mu$ for a narrow-stripe LOC and $20\sim30\,\mu$ for a regular narrow-stripe DH. The less curved wave front (larger radius of curvature) of the narrow-stripe LOC hints at the formation of an index waveguide.[3] We attribute the nature of the index waveguide to a thermally induced refractive index distribution across the stripe. Additional experimental evidence can be found from the result of a time-resolved near-field measurement, as shown in Fig. 2. One can see that, as a current pulse is applied, the beam-width reduction takes place over a ~ 1-μs period. In the meantime the laser output pulse exhibits appreciable distortion due to delayed turn-on. A similar narrowing effect is also observed in the far-field pattern. The transition time of $\sim 1\,\mu$s indicates that the waveguiding mechanism is most likely thermal in origin. In a narrow-stripe LOC, thermal effects are expected to be more important because of the high threshold current density resulting from the lower confinement factor and from higher absorption loss (having a $\Gamma^{-1/4}$ dependence of the lateral mode spreading[4]). The lateral waveguiding due to gain variation is a relatively weak mechanism and can be greatly perturbed by thermally induced changes in the real part of the refractive indices of all the layers in the LOC waveguide. We note that the derivative of index with temperature is positive for AlGaAs, causing index guiding to occur with a temperature maximum under the center of the stripe. Carrier-induced antiguiding of the mode is reduced because the carriers are localized in the active layer. Since the carrier density is higher, while the confinement factor is lower, we expect that the antiguiding effects in the LOC laser will be comparable to those in the DH. The larger current densities in the LOC should cause more local heating and index guiding.

A direct consequence of the formation of the thermal waveguide is the lower cw threshold current and delayed turn-on when a long current pulse is applied. We have found that the near-field beam width continues to decrease even above the threshold as shown in Fig. 1. As a result, the mode loss average over the beam cross section decreases with increasing current. This nonlinear behavior with current could explain the anomalously high differential quantum efficiency of the cw P-I characteristics.

The filamentlike emission of narrow-stripe LOC also acts to promote self-sustained oscillations which are rarely observed among regular narrow-stripe DH lasers before aging. The reduction of the beam width concentrates the mode power to the center of the stripe and, therefore, enhances the carrier depletion in the center of the gain profile. It has been shown that the carrier-depletion-induced self-focusing acts to reduce the damping of relaxation oscillation and thus promote sustained oscillation.[5,6] We have indeed observed the oscillation of the near-field beam width, accompanying the pulsating laser output, in our time-resolved near-field measurement, as shown in Fig. 2. This is consistent with that described in Ref. 6.

The increasing positive index guide also causes the astigmatism to increase. The astigmatism D of Gaussian beams, defined as the location of the virtual source behind the facet, can be related to the radius of curvature R of the wave front and the near-field beam width W by

$$D=\left(\frac{\pi W^2}{\lambda}\right)^2\frac{R}{R^2+(\pi W^2/\lambda)^2}, \tag{1}$$

where λ is the wavelength of the beam. The relationship can be deduced from Eq. (2.35) and (2.36) of Ref. 3. For truly index-guided lasers, the radius of curvature is infinite and the astigmatism approaches zero. However, for most narrow-stripe devices, $R^2 \ll (\pi W^2/\lambda)^2$ and therefore $D \approx R$. Thus, the astigmatism becomes larger with increasing contribution of the thermally induced index guide.

We have shown that the differences between narrow-stripe DH lasers and narrow-stripe LOC lasers can be qualitatively explained in terms of a thermal waveguide effect. Our analysis suggests that thermal effects are important factors to be considered in understanding and controlling the characteristics of gain-guided lasers, particularly aged devices in which higher heat dissipation can take place due to increasing rate of nonradiative recombination. Statistically, we have found that the development of sustained oscillations of regular narrow-stripe lasers after aging is highly correlated with the narrowing of the near field and far field, which implies a less curved wave front. In lasers which exhibit significant far-field narrowing, the astigmatism is also higher than normal. When driven by a long current pulse, the light output exhibits noticeable pulse distortion over a 1-μs period of the type shown in Fig. 2. These phenomena are strikingly similar to those observed in narrow-stripe LOC lasers and can be explained in terms of a thermal waveguide effect described in this letter.

The authors wish to thank Dr. P. S. Zory for helpful

discussions and comments, and H. Vollmer and J. Duda for technical assistance.

[1]H. F. Lockwood, H. Kressel, H. S. Sommers, and F. Z. Hawylo, Appl. Phys. Lett. **17**, 499 (1970).
[2]Y. C. Chen (unpublished).
[3]D. D. Cook and F. R. Nash, J. Appl. Phys. **46**, 1660 (1975).
[4]T. L. Paoli, IEEE J. Quantum Electron. **QE-13**, 662 (1977).
[5]R. Lang, Jpn. J. Appl. Phys. **19**, L93 (1980).
[6]J. P. van der Ziel, IEEE J. Quantum Electron. **QE-17**, 60 (1981).

Discrete Fourier transformation using a time-integrating, acousto-optical signal processor

John N. Lee, Shih-Chun Lin, and A. B. Tveten
Naval Research Laboratory, Washington, D.C. 20375

(Received 15 February 1982; accepted for publication 28 April 1982)

Discrete Fourier transformation has been implemented on a time-integrating, acousto-optical signal processor based on the chirp z-transform algorithm. Novel features are the use of an injection diode laser for signal input and an additive architecture. The operational principles are analytically derived and experimentally demonstrated. Discrete Fourier transforms of 4, 8, 64, and 128 points are in excellent agreement with fast Fourier transform simulations. The architecture lends itself easily to miniaturization and to extension to parallel, multichannel operation.

PACS numbers: 42.30.Kq, 42.60.Kg

In many applications, such as in the fields of radar and sonar, large-bandwidth Fourier transforms over discrete spatial and temporal variables must be obtained before useful information can be extracted. Acousto-optical processing is particularly suitable for this purpose when a chirp z-transform algorithm is used. The definition of the discrete Fourier transform (DFT) of a sampled data stream, $S_n(t)$, is

$$F(k) = \sum_{n=0}^{N-1} S_n(t) \exp\frac{-2\pi i n k}{N}. \quad (1)$$

By the substitution of the identity $nk = (1/4)[n+k)^2 - (n-k)^2]$ in the exponential term, one obtains

$$F(k) = \sum_{n=0}^{N-1} S_n(t) \exp\left(\frac{i\pi(n-k)^2}{2N}\right) \exp\left(\frac{-i\pi(n+k)^2}{2N}\right). \quad (2)$$

This algorithm is also known as the triple-product convolver (TPC) implementation of the DFT,[1] since the terms in Eq. (2) are products of three factors. The exponential terms can be generated in acousto-optic cells using linear-FM rf signals. There exists a variety of arrangements for performing the required multiplication[2] and summation. A space-integrating scheme has been used[3] to obtain $F(k)$, where the data $S_n(t)$ are carried by individual light beams. In general, the data $S(t)$ can be impressed onto the optical beam via direct modulation of a diode laser, which offers compact size and high efficiency. In this letter, we report an additive, time-integrating scheme different from the multiplicative ones described in Ref. 2. Our experimental results demonstrated, for the first time, that the optical processor, using a modulated diode laser source can be used to compute DFT's of up to128 sampled points.

The core of the optical signal processor is the modified Mach–Zehnder interferometer as shown in Fig. 1. The optical output of a diode laser, after collimation, is split into two beams of equal intensity by the first beam splitter. Each beam is then directed through a Bragg cell. In this implementation of the Fourier transformation, the Bragg cells are driven in the opposite directions by the same linear FM (chirped) rf waves. The Bragg-diffracted optical waves will be phase modulated to yield the two exponential terms of opposite delays. The diode laser is intensity modulated by the signal $S(t)$. When the two diffracted fields are mixed in the square-law detector array and time integrated over a period of T, the electrical charge from the detector array consists of three terms: two bias terms proportional to intensities of the optical beams in the two legs of the interferometer, and a cross term containing the desired Fourier transform of the signal modulating the diode laser. Assuming that the path lengths and optical intensities in the two legs of the interferometer have been made equal, then the charge representing

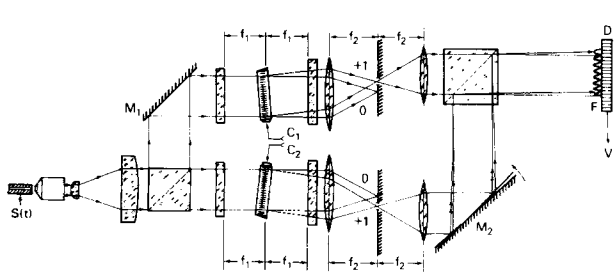

FIG. 1. Experimental arrangement for time-integrating, acousto-optic DFT processor.

 0003-6951/82/02131-03$01.00